

Crust-core coupling in rotating neutron stars

Kostas Glampedakis and Nils Andersson

School of Mathematics, University of Southampton, Southampton SO17 1BJ, UK

(Dated: November 17, 2018)

Motivated by their gravitational-wave driven instability, we investigate the influence of the crust on r-mode oscillations in a neutron star. Using a simplistic model of an elastic neutron star crust with constant shear modulus, we carry out an analytic calculation with the main objective of deriving an expression for the “slippage” between the core and the crust. Our analytic estimates support previous numerical results, and provide useful insights into the details of the problem.

I. INTRODUCTION

The study of neutron star oscillation modes has long been a vivid research area, attracting additional attention in recent years after the discovery that inertial modes of rotating fluid stars are prone to unstable behaviour when coupled to gravitational radiation [1, 2]. This instability is characterised by growth timescales short enough to make it astrophysically relevant. For example, unstable r-modes (the class of purely axial inertial modes) have been proposed as a possible mechanism for limiting the spin-periods of neutron stars in Low-Mass X-ray Binaries (LMXBs) and as a potential source of gravitational radiation for the ground-based detectors. For a detailed review of the r-mode instability we refer the reader to Ref. [3].

Studies of the r-mode instability have revealed a host of possible damping mechanisms counteracting the growth of an unstable mode. Among the most efficient is the damping due to friction, via the formation of an Ekman boundary layer at the crust-core interface, see [4] for a recent discussion. For mature neutron stars, this mechanism could be the key damping agent for unstable r-modes. The crust forms once the star cools below 10^{10} K or so, soon after the star is born. At the temperatures relevant for a mature neutron star, the heavy constituents in the core (neutrons, protons, hyperons) are expected to be in a superfluid/superconducting state. This leads to the suppression of, for example, the hyperon bulk viscosity [5, 6, 7] and the emergence of mutual friction (see also [8] for a recent discussion of the shear viscosity in a superfluid neutron star core). In this paper we focus on the role of the crust. A detailed discussion of the natural first approximation, where the crust is modelled as a rigid spherical “container”, and the viscous Ekman layer that forms at the core-crust interface, can be found in [4].

In the present paper we explore a different aspect of the problem, namely, we consider a more refined model with an elastic crust characterised by a finite shear modulus. A model along these lines was considered by Lee & Strohmayer [9] (hereafter LS) in their numerical study of oscillating neutron stars (for some earlier studies see [10] and [11]). Being elastic, the crust can sustain forced oscillations driven by (say) a core mode. In addition the crust has its own unique dynamics, with a set of oscillation modes associated with the elasticity. The problem becomes very rich since one expects resonances/avoided crossings to take place when a core-mode frequency approaches a crust-mode frequency [12], for example as the star spins down. This picture is certainly much more complicated than one with the fluid simply “rubbing” against a rigid boundary wall.

If we model the crust in a more sophisticated manner we should also expect the relevant r-mode damping timescales to be altered. This was emphasised by Levin & Ushomirsky (hereafter LU) [13] who used the formalism of LS but considered the simpler case of a uniform density, slowly rotating spherical star, with a constant shear-modulus crust. They argue that the change in the r-mode damping timescale, compared to the solid crust case, can be quantified in terms of the relative motion between the crust and the core. Introducing the dimensionless “slippage” $\mathcal{S}_c = (v - v_0)/v_0$, where v is the core fluid velocity immediately beneath the crust and v_0 is the corresponding velocity in a fluid star, LU argue that an approximate revised damping timescale is the standard Ekman result multiplied by the factor $1/\mathcal{S}_c^2$. LU attacked the problem by direct numerical integration of the crust-core equations, and showed that the slippage is $\mathcal{S}_c \approx 0.05 - 0.1$ in a typical case. Hence, they found that the r-mode damping timescale could be more than 100 times slower than for a solid crust. For rotation rates such that the inertial r-mode frequencies are close to the various shear modes in the crust, the slippage factor can however become much larger (of order unity). These results were confirmed in a later study by Yoshida and Lee [12].

Our aim in this paper is to study the interaction between the oscillating fluid core and the crust using purely analytical tools. Our decision to pursue the problem analytically was driven by a desire to obtain a better understanding of the intricate coupling to the crust, and the way that the final result scales with the different parameters. Although our chosen strategy leads to a significant amount of algebra, we believe that the end result justifies the effort. Certainly, the analytical relations we derive illustrate the underlying physics much clearer than a direct numerical calculation would. To achieve our aims, we make use of boundary-layer theory [4] combined with a truncated expansion in spherical harmonics for the perturbed fluid variables. In order to keep the calculation tractable, we consider a uniform

density, slowly rotating Newtonian star with a constant shear modulus crust. We study in detail how the crust is driven by a single r-mode in the core, and then compute the slippage and the induced modifications to the r-mode. Our formulation of the problem is very similar to that of LU. The main difference is that we assume that a purely axial r-mode in the core acts as the driving force, while LU included $\mathcal{O}(\Omega^2)$ (polar) corrections to their core mode (Ω is the rotation rate). Our study is also limited to a crust with a relatively small shear modulus (more like a jelly than a solid). In this sense our analysis is less general than that of LU [13], but we show that realistic estimates of the shear modulus support our assumptions. Where both calculations are valid, our results are in good agreement with those of LU (they are not identical due to the slightly different formulations of the problem).

The paper is organised as follows. In Section II we briefly discuss the elastic character of the crust, providing some justification for our assumption of a constant shear modulus. The main scope of the paper is developed in Section III where we discuss neutron stars with elastic crusts, and study the delicate coupling between the core-flow and the crust. The concluding Sections, IV & V, of the paper provide a discussion of the physical relevance of our results and a summary. In these sections we compare our results to previous work on this problem. We also point out interesting extensions of the present work.

Aware of the somewhat heavy algebra involved in our analysis, we have made an effort to make the sections discussing the results self-contained. This should make the results accessible also for readers who are not prepared to bear with us as we work through the details of the core-crust problem. Many of the technical details of our calculation are located in the Appendices.

II. MODELLING THE NEUTRON STAR CRUST

We first discuss in some detail the properties of an elastic neutron star crust. This is the case that is relevant for most neutron stars since the crust is thought to form already at temperatures near 10^{10} K, possibly within minutes after the neutron star is born. Furthermore, the crust is not expected to be particularly rigid. Even though it supports shear stresses its nature is more like jelly, and one would expect it to take part in any global oscillation of the star. In addition, it will support distinct crust modes characterised by the speed of shear waves in the nuclear lattice.

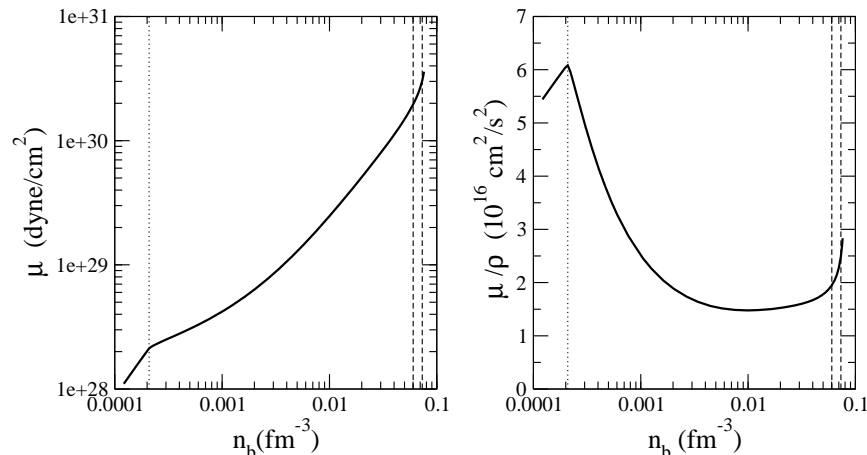


FIG. 1: The shear modulus, based on Eq. (1) and data for the equation of state of Douchin and Haensel [14]. The vertical dotted line indicates the location of neutron drip, while the dashed lines indicate the region near the base of the crust where the nuclei undergo a series of changes in shape, cf. the discussion in [14].

In order to keep the problem analytically tractable, we will adopt a simple uniform density neutron star model. In addition, we will take the fluid to be inviscid since we are mainly interested in the mechanical, dissipation free, coupling between the r-mode and the crust. Furthermore, we assume that the crust is characterised by a *uniform* shear modulus μ . This assumption (which was also adopted by LU [13]) is somewhat unrealistic [9], but it greatly simplifies the analysis. A study of the non-isotropic case requires a numerical solution. On the other hand, realistic models for the crust suggest that the speed of shear waves is remarkably constant throughout the crust. We illustrate this in Figure 1 where we have combined the standard expression for the shear modulus of a *bcc* lattice

$$\mu = 0.3711 \frac{Z^2 e^2 n_N^{4/3}}{2^{1/3}} \quad (1)$$

where Z is the number of protons per nucleus and n_N is the number density of nuclei, with the data for the recent equation of state of Douchin and Haensel [14]. As is clear from this figure the ratio

$$\tilde{\mu} = \frac{\mu}{\rho} \approx 10^{16} \text{ cm}^2/\text{s}^2 \quad (2)$$

only varies by a factor of a few in the crust. It should also be noted that μ does not vanish at the core-crust phase-transition. Given the results shown in Figure 1 it is clearly not too unreasonable to treat $\tilde{\mu}$ as a constant.

The crust's rigidity can be quantified by means of the ratio (essentially the ratio between the speed of shear waves and a characteristic rotation velocity, or the relation between the elasticity and the Coriolis force),

$$\Lambda \equiv \frac{\tilde{\mu}}{R^2 \Omega^2} \quad (3)$$

The crust behaves almost like a fluid when $\Lambda \ll 1$ and is essentially rigid in the opposite limit. In the present work we will only be concerned with the former limit. In this sense, our analysis is less general than that of LU who put no restrictions on the ratio (3). Introducing a characteristic rotation frequency

$$\Omega_0^2 = \frac{GM}{R^3} \rightarrow \Omega_0^2 R^2 \approx 10^{20} \text{ cm}^2/\text{s}^2 \quad (4)$$

(such that the Kepler break up rotation rate is about $0.6\Omega_0$) we see that we will have

$$\Lambda \approx 10^{-4} \left(\frac{\Omega_0}{\Omega} \right)^2 \quad (5)$$

This clearly shows that the $\Lambda \ll 1$ limit is appropriate provided that we do not let $\Omega \rightarrow 0$. In a sense, this illustrates the fact that our calculation is limited to rotating stars. Another reason for this is that we will assume that the core fluid undergoes an inertial r-mode oscillation. This would not make sense for a non-rotating star as these modes then become trivial.

III. CRUST-CORE COUPLING

A. Formulating the problem

The physical situation we wish to examine is that of a single core r-mode coupled to the crust. As a result of this coupling the crust will oscillate. At the same time there will be some ‘‘back-reaction’’ on the core mode. Mathematically, one needs to solve the Euler equation in the core region, and the corresponding equations for an elastic body in the crust region. Boundary conditions need to be imposed at the core-crust interface and at the star's surface and centre. Our aim is to approach the problem through a two-parameter expansion: a slow rotation expansion in Ω/Ω_0 together with an expansion in Λ . The discussion in the previous Section illustrates the reason why this is a tricky problem. Yet we will see that we can make significant (possibly surprising) progress by combining these expansions with boundary layer techniques.

We assume a uniform density, incompressible fluid. Since we work at leading order in rotation we can assume our star to be spherical. Moreover, we adopt the so-called Cowling approximation where the perturbation in the gravitational potential is ignored. This is a sensible assumption, since for the quasi-axial modes we are interested in the associated density perturbation (and consequently the perturbation in the gravitational potential) is a higher order correction. In the rotating frame, the linearised Euler and continuity equations for the crust flow are

$$\partial_t^2 \xi + 2\mathbf{\Omega} \times \partial_t \xi = -\frac{1}{\rho} \nabla \delta p + \tilde{\mu} \nabla^2 \xi \quad (6)$$

$$\nabla \cdot \xi = 0 \quad (7)$$

where we have taken $\tilde{\mu} = \mu/\rho = \text{constant}$. For the present problem it is natural to work with the displacement vector ξ . The main reason for this is that the shear introduces a Hookean restoring force into the Euler equations, i.e. terms $\sim \mu \nabla^2 \xi$ [9, 10, 11]. The core flow is described by the $\mu \rightarrow 0$ limit of the above equations.

We assume a decomposition of the form,

$$\xi = \frac{1}{r} \sum_{l \geq m} \left[W_l Y_l^m \hat{\mathbf{e}}_{\mathbf{r}} + \left(V_l \partial_\theta Y_l^m - i \frac{U_l \partial_\varphi Y_l^m}{\sin \theta} \right) \hat{\mathbf{e}}_\theta + \left(\frac{V_l \partial_\varphi Y_l^m}{\sin \theta} + i U_l \partial_\theta Y_l^m \right) \hat{\mathbf{e}}_\varphi \right] e^{i\sigma t} \quad (8)$$

where the relative phase between the polar $\{W_l, V_l\}$ and axial components $\{U_l\}$ is chosen such that the final perturbation equations are real valued. We also decompose the perturbed pressure as

$$\frac{\delta p}{\rho} = \sum_{l \geq m} h_l Y_l^m \quad (9)$$

The three components of the Euler equation (6) then reduce to (in the following, a prime denotes a radial derivative);

$$\mathcal{E}^r = \sum_{l \geq m} \left[\left\{ r h_l' - \sigma^2 W_l + 2m\sigma\Omega V_l \right\} Y_l^m + 2\sigma\Omega U_l \sin\theta \partial_\theta Y_l^m + \tilde{\mu} \left\{ 2\frac{W_l}{r^2} - W_l'' + l(l+1)\frac{W_l - 2V_l}{r^2} \right\} Y_l^m \right] = 0 \quad (10)$$

$$\begin{aligned} \mathcal{E}^\theta = \sum_{l \geq m} & \left[-m\sigma^2 U_l Y_l^m + \{h_l - \sigma^2 V_l\} \sin\theta \partial_\theta Y_l^m + 2m\sigma\Omega V_l \cos\theta Y_l^m + 2\sigma\Omega U_l \cos\theta \sin\theta \partial_\theta Y_l^m \right. \\ & \left. - m\tilde{\mu} \left\{ U_l'' - l(l+1)\frac{U_l}{r^2} \right\} Y_l^m - \tilde{\mu} \left\{ V_l'' - l(l+1)\frac{V_l}{r^2} + 2\frac{W_l}{r^2} \right\} \sin\theta \partial_\theta Y_l^m \right] = 0 \end{aligned} \quad (11)$$

$$\begin{aligned} \mathcal{E}^\varphi = \sum_{l \geq m} & \left[\{m h_l + 2\sigma\Omega W_l - m\sigma^2 V_l\} Y_l^m - \sigma^2 U_l \sin\theta \partial_\theta Y_l^m + 2m\sigma\Omega U_l \cos\theta Y_l^m + 2\sigma\Omega V_l \cos\theta \sin\theta \partial_\theta Y_l^m \right. \\ & \left. - 2\sigma\Omega W_l \cos^2\theta Y_l^m - m\tilde{\mu} \left\{ V_l'' - l(l+1)\frac{V_l}{r^2} + 2\frac{W_l}{r^2} \right\} Y_l^m - \tilde{\mu} \left\{ U_l'' - l(l+1)\frac{U_l}{r^2} \right\} \sin\theta \partial_\theta Y_l^m \right] = 0 \end{aligned} \quad (12)$$

These equations are identical to those given in [9, 11], specialised for constant shear modulus and incompressible flow.

As discussed by Lee & Strohmayer [9] it is convenient to consider two particular combinations of the above equations. The first is the radial component of the vorticity,

$$m\mathcal{E}^\theta - \sin\theta \partial_\theta \mathcal{E}^\varphi = 0 \quad (13)$$

and the second is the ‘‘divergence equation’’,

$$\sin\theta \partial_\theta \mathcal{E}^\theta - m\mathcal{E}^\varphi = 0 \quad (14)$$

From eqn. (13) and from the combination of eqns. (14) and (10) we arrive at the following equations,

$$\begin{aligned} & \frac{\sigma}{2\Omega} \left[l(l+1)\frac{\sigma}{2\Omega} - m \right] U_l + \frac{\sigma}{2\Omega} \left[(l+1)Q_l \{W_{l-1} - (l-1)V_{l-1}\} - lQ_{l+1} \{W_{l+1} + (l+2)V_{l+1}\} \right] \\ & + l(l+1)\frac{\tilde{\mu}}{4\Omega^2} \left[U_l'' - l(l+1)\frac{U_l}{r^2} \right] = 0 \end{aligned} \quad (15)$$

$$\begin{aligned} & \frac{\sigma}{2\Omega} \left[l(l+1)\{(l-1)Q_l U_{l-1} - (l+2)Q_{l+1} U_{l+1}\} - (l-1)(l+1)Q_l r U_{l-1}' - l(l+2)Q_{l+1} r U_{l+1}' - m\{rV_l' - W_l\} \right] \\ & + l(l+1) \left(\frac{\sigma}{2\Omega} \right)^2 [rV_l' - W_l] + l(l+1)\frac{\tilde{\mu}}{4\Omega^2} \left[rV_l''' - 2W_l'' + (l-1)(l+2)\frac{W_l}{r^2} \right] = 0 \end{aligned} \quad (16)$$

where

$$Q_l = \sqrt{\frac{(l+m)(l-m)}{(2l-1)(2l+1)}} \quad (17)$$

The continuity equation (7) provides one additional expression

$$(rW_l)' - l(l+1)V_l = 0 \quad (18)$$

Equations (15), (16) and (18) are the basic equations for our problem. They involve only the eigenfunctions of ξ and the frequency σ and are equivalent to the initial Euler equations. It is interesting to note that our equations only couple multipoles of order l to those corresponding to $l \pm 1$. This is in contrast to the (fluid) equations used by eg. Lockitch and Friedman [15] to study inertial modes, where coupling to $l \pm 2$ multipoles was also present. In this sense, the present set of equations is simpler and could possibly be advantageous also in studies of the fluid inertial mode problem.

B. Boundary conditions

The dynamical equations are accompanied by boundary conditions at the crust-core interface (at $r = R_c$) and at the surface of the star ($r = R$). These boundary conditions can be formulated in terms of the traction components [9, 16],

$$T_r = 2\mu\partial_r\xi^r - \Delta p \quad (19)$$

$$T_\theta = \mu \left[\partial_r\xi^\theta - \frac{1}{r}\xi^\theta + \frac{1}{r}\partial_\theta\xi^r \right] \quad (20)$$

$$T_\varphi = \mu \left[\partial_r\xi^\varphi - \frac{1}{r}\xi^\varphi + \frac{1}{r\sin\theta}\partial_\varphi\xi^r \right] \quad (21)$$

where Δp is the Lagrangian variation in the pressure. The traction vector is constructed by projecting the fluid stress tensor along the unit normal vector at the interface, and represents the force per unit area. Perturbing (in the Lagrangian sense) this projection results in the expressions above.

At the crust-core interface all traction components as well as the radial displacement vector need to be continuous. Specifically, this requirement leads to (after setting $l = m$ in the axial component)

(i) Vanishing tangential traction at the interface and surface:

$$\tilde{\mu}[rU'_m - 2U_m] = 0 \quad \text{at } r = R_c, R \quad (22)$$

$$\tilde{\mu}[rV'_{m+1} + W_{m+1} - 2V_{m+1}] = 0 \quad \text{at } r = R_c, R \quad (23)$$

(ii) Continuity of the radial traction at the interface:

$$\delta p^{\text{core}} = \delta p^{\text{crust}} - 2\mu\partial_r\xi^r \quad \Rightarrow \quad h_{m+1}^{\text{core}} = h_{m+1}^{\text{crust}} - 2\tilde{\mu} \left(\frac{W_{m+1}}{r} \right)' \quad \text{at } r = R_c \quad (24)$$

(iii) Vanishing of the radial traction at the surface:

$$\delta p + \xi^r \nabla_r p - 2\mu\partial_r\xi^r = 0 \quad \Rightarrow \quad R^2 h_{m+1} = -g_0 R W_{m+1} + 2\tilde{\mu}[R W'_{m+1} - W_{m+1}] \quad \text{at } r = R \quad (25)$$

where we have defined $g_0 = GM/R^2$, the surface gravitational acceleration (which appears after using the background Euler equation $\nabla p = -\rho\nabla\Phi$). One can show that this final condition reduces to the standard condition of vanishing Lagrangian pressure perturbation at the surface in the limit $\tilde{\mu} \rightarrow 0$.

(iv) Continuity of the radial displacement at the interface:

$$W_{m+1}(R_c^-) = W_{m+1}(R_c^+) \quad (26)$$

In addition, we require all core flow variables to be finite at $r = 0$.

C. Simple mode solutions?

Before we begin our main analysis, it is worth discussing the nature of some comparatively simple solutions. First of all, we ought to be able to reproduce the standard fluid r-mode solution from equations (15) and (16). Let $\tilde{\mu} = 0$ and assume that the only non-vanishing displacement is U_m . Then eqn. (15) with $l = m$ leads to

$$[m(m+1)\sigma^2 - 2m\sigma\Omega] U_m = 0 \quad (27)$$

and we must clearly have either $\sigma = 0$ or

$$\sigma = \frac{2\Omega}{m+1} \quad (28)$$

which is the standard result. Meanwhile eqn. (16) with $l = m - 1$ is trivially satisfied since $Q_m = 0$. Finally we need eqn (16) with $l = m + 1$;

$$rU'_m - (m+1)U_m = 0 \quad \Rightarrow \quad U_m = Ar^{m+1} \quad (29)$$

which is the expected eigenfunction.

Given the perturbation equations from the previous section it is also easy to prove that inertial modes in uniform density stars cannot have polar terms as their highest multipole contribution [15]. Consider a mode which truncates after $l = n$ (say) and for which the n^{th} terms are polar. Then eqn. (15) with $l = n + 1$ provides the relation

$$W_n - nV_n = 0 \quad (30)$$

Combining this with the continuity equation we see that we must have

$$W_n = r^n \quad (31)$$

which cannot satisfy the required surface boundary condition $W_n(R) = 0$. In other words, the highest multipole term of an inertial-mode solution cannot be polar.

More important for the present investigation is to ask whether we can have purely axial modes in a star with a fluid core and an elastic crust. We have already shown that in order to have only U_m (say) nonzero in the fluid core, we must have a mode with the r-mode frequency. We also have the eigenfunction from Eq. (16). In order to be consistent, this eigenfunction must satisfy the remaining part of Eq. (15) in the crust, i.e.

$$U_m'' - m(m+1)\frac{U_m}{r^2} = 0 \quad (32)$$

This is, in fact, the case. But our solution is nevertheless not acceptable because it cannot satisfy the boundary conditions of vanishing traction at the base of the crust and the surface of the star [Eq. (22) above]. We require

$$U_m' - 2\frac{U_m}{r} = 0 \quad \text{at} \quad r = R_c \quad \text{and} \quad r = R \quad (33)$$

which clearly is incompatible with our solution. Thus we conclude that *a purely axial mode is no longer possible in the presence of the crust.*

This is, in fact, a bit puzzling because we can extend the argument to demonstrate that a crust mode with only $[U_m, V_{m+1}, W_{m+1}] \neq 0$ is also inconsistent! This would seem to cast some doubt on the numerical results of LU [13] who only include these terms. In reality the situation is a bit more complex. As also mentioned by Lee and Strohmayer [9], the problem should be approached in a way similar to the inertial-mode problem for a fluid star [15]. Even though one should not at the outset restrict the number of multipoles included in the calculation one will always in practise truncate after some multipole. Since this involves neglecting some of the relations implied by the recurrence relations it renders the solution somewhat inconsistent (as in the case of LU). However, one would expect the mode-solution to converge when more multipoles are accounted for, and it does not seem unreasonable to expect that a lower order representation will be fairly accurate. Indeed, this turns out to be the case in a similar calculation for the standard Ekman layer problem where the known exact solution is quite well approximated by a $[U_m, V_{m+1}, W_{m+1}]$ truncated representation (see [4] for discussion). As we are seeking an analytical approximation to the solution, it is natural to truncate the solution at the simplest "meaningful" level. This is an obvious weakness of our analysis. A more detailed study, investigating for example the convergence as more multipoles are accounted for and whether the outcome depends on the parameter values, requires a numerical solution.

D. Core flow

As we have mentioned, we will assume that the bulk core flow is described by a single $l = m$ r-mode, which is capable of penetrating the crust region and driving the flow there. In return, it picks up corrections due to the coupling with the crust. Furthermore, we will truncate the multipolar expansion (see eqn. (8)) at the level $\{U_m, V_{m+1}, W_{m+1}\}$. Note that the same truncation was adopted in previous studies of the problem [9, 13].

For the dynamical variables we assume expansions of the form

$$Q = Q^0 + Q^1 + Q^2 + \dots \quad (34)$$

where, for brevity, we have collectively denoted $Q = \{U_m, V_{m+1}, W_{m+1}, h_{m+1}, \sigma\}$. Expansion (34) has no obvious small parameter in it; it is written anticipating the fact that there is a one to one correspondence with the similar expansion in the crust region (which has the well defined expansion parameter $\tilde{\mu}$, see Section III E). The reason for including terms up to second order will become apparent in the discussion of the crust flow.

As we are assuming an r-mode solution at leading order we take the leading order polar pieces to be zero, i.e.

$$W_{m+1}^0 = V_{m+1}^0 = 0 \quad (35)$$

The non-zero axial piece is normalised in such a way that $A = 1$ in (29), i.e. $U_m^0 = R_c^{m+1}$ at the base of the crust.

The next step is to insert the expansion (34) in the main equations (15)-(18). The resulting first and second order equations are listed in Appendix A. The analysis in that Appendix provides the results,

$$V_{m+1}^1 = \frac{\sigma_1}{2\Omega}(m+1)Q_{m+1}r^{m+1} \quad (36)$$

$$W_{m+1}^1 = (m+1)V_{m+1}^1 \quad (37)$$

$$U_m^1 = \gamma r^{m+1} \quad (38)$$

and

$$V_{m+1}^2 = \frac{[\sigma_2 + \gamma\sigma_1]}{2\Omega}(m+1)Q_{m+1}r^{m+1} \quad (39)$$

$$W_{m+1}^2 = (m+1)V_{m+1}^2 \quad (40)$$

$$U_m^2 = \delta r^{m+1} \quad (41)$$

where γ and δ are constants.

These results demonstrate the importance of the frequency corrections σ_1 and σ_2 . Had we neglected them, we would have effectively killed all corrections to the core flow. Hence, the secondary core flow is linked to the crust-induced correction to the mode oscillation frequency.

Finally, we need to calculate the pressure correction, anticipating the fact that the pressure appears explicitly in some of the boundary conditions. For this purpose it is convenient to use the \mathcal{E}^θ component of the Euler equation, eqn. (11). We easily obtain,

$$h_{m+1}^0 = -\frac{mQ_{m+1}}{(m+1)^2}r^{m+1} \quad (42)$$

$$h_{m+1}^1 = -\frac{4\Omega^2 Q_{m+1}}{(m+1)^2} \left[\frac{\sigma_1}{2\Omega}(m+1)(2m-1) + m\gamma \right] r^{m+1} \quad (43)$$

$$h_{m+1}^2 = -\frac{4\Omega^2 Q_{m+1}}{(m+1)^2} \left[(m+1)(2m-1)\frac{\sigma_2 + \gamma\sigma_1}{2\Omega} + m\delta + (m-2)(m+1)^2 \left(\frac{\sigma_1}{2\Omega} \right)^2 \right] r^{m+1} \quad (44)$$

In the end, all core-flow eigenfunctions (up to second order) are expressed in terms of the (as yet unknown) parameters σ_1 , σ_2 , γ and δ . As we will see, these are linked to the crust flow through the interface conditions.

E. Crust flow: setting up the equations

In the crust region the Euler equations have additional term of form $\tilde{\mu}\nabla^2\xi$. These terms are similar to the viscous terms in the Ekman layer problem [4], but here they represent the crust's elastic restoring force. Despite the additional terms being dissipative in one case and oscillatory in the other, the problems are mathematically similar. The crust equations are likely to exhibit "boundary layer behaviour" when the coefficient $\tilde{\mu}$, which multiplies the highest order spatial derivatives, is treated as a small parameter (i.e. in the limit $\Lambda \ll 1$). This feature will turn out to be of key importance when solving the equations.

Since we are only considering an "almost fluid" crust, one would expect the crust flow to be primarily axial in nature. as it is driven by the quasi-axial core oscillation. In the crust, as in the core, we assume from the outset that V_{m+1} and W_{m+1} vanish at leading order, and truncate the multipole expansion (8) by including only the $\{U_m, V_{m+1}, W_{m+1}\}$ eigenfunctions.

In the crust, the continuity equation (18) with $l = m + 1$, gives

$$(rW_{m+1})' = (m+1)(m+2)V_{m+1} \quad (45)$$

Meanwhile (15) with $l = m$, and (16) with $l = m + 1$, can be written

$$\frac{\sigma}{2\Omega} \left[(m+1)\frac{\sigma}{2\Omega} - 1 \right] U_m + \frac{\tilde{\mu}}{4\Omega^2}(m+1) \left[U_m'' - m(m+1)\frac{U_m}{r^2} \right] - \frac{\sigma}{2\Omega}Q_{m+1}[W_{m+1} + (m+2)V_{m+1}] = 0 \quad (46)$$

$$\frac{\sigma}{2\Omega} m [(m+1)(m+2)Q_{m+1}U_m - (m+2)Q_{m+1}rU'_m - rV'_{m+1} + W_{m+1}] + \left(\frac{\sigma}{2\Omega}\right)^2 (m+1)(m+2) [rV'_{m+1} - W_{m+1}] + \frac{\tilde{\mu}}{4\Omega^2} (m+1)(m+2) \left[rV'''_{m+1} - 2W''_{m+1} + m(m+3)\frac{W_{m+1}}{r^2} \right] \quad (47)$$

We now adopt a standard uniform expansion [17],

$$Q = Q^0 + \tilde{Q}^0 + \tilde{\mu}^a \{Q^1 + \tilde{Q}^1\} + \tilde{\mu}^{2a} \{Q^2 + \tilde{Q}^2\} + \mathcal{O}(\tilde{\mu}^{3a}) \quad (48)$$

where we have again used the collective notation $Q = \{U_m, V_{m+1}, W_{m+1}, h_{m+1}, \sigma\}$. “Boundary layer” variables are denoted by tildes (and for them we assume dominant radial derivatives $\partial_r \sim \mathcal{O}(\tilde{\mu}^{-a})$). The remaining quantities pertain to the smoothly varying, background crust flow. Note that in (48) the power-law exponent a is initially undetermined. Its value is fixed by the equations themselves, in order for them to make sense. The analysis of Appendix B shows that $a = 1/2$.

Inserting the expansion (48) in eqns. (45)–(47) we find two families of equations, one for the “boundary layer” and one for background variables. We derive all the dynamical equations required for the determination of the crust flow up to $\mathcal{O}(\tilde{\mu})$ (the reason for pursuing the calculation to this order, rather than simply to $\mathcal{O}(\tilde{\mu}^{1/2})$ will become apparent below). Next, we expand the various boundary conditions (22)–(26). In order to avoid overloading the reader with algebra we carry out these calculations in Appendices B and C.

1. Leading-order flow

Having written down all the relevant equations, we can now solve eqns. (B10) and (B15) for the leading order flow. After decoupling these equations we end up with,

$$\tilde{\mu}^2 \tilde{V}_{m+1}^{0''''} + \frac{8\Omega^2 \tilde{\mu}}{(m+1)^2(m+2)} \tilde{V}_{m+1}^{0''} - \frac{16\Omega^4 m(m+2)}{(m+1)^4} Q_{m+1}^2 \tilde{V}_{m+1}^0 = 0 \quad (49)$$

Trying the Ansatz, $\tilde{V}_{m+1}^0 \sim e^{\lambda(r-R_c)}$ we find for the exponent a pair of real and a pair of imaginary roots,

$$\lambda_{1,2} = \pm \frac{2\Omega}{\tilde{\mu}^{1/2}} \left(\frac{\sqrt{\alpha} - 1}{(m+2)(m+1)^2} \right)^{1/2} \quad (50)$$

$$i\lambda_{3,4} = \pm \frac{2\Omega}{\tilde{\mu}^{1/2}} \left(\frac{\sqrt{\alpha} + 1}{(m+2)(m+1)^2} \right)^{1/2} \quad (51)$$

where

$$\alpha = 1 + m(m+2)^3 Q_{m+1}^2 \quad (52)$$

The occurrence of purely real and imaginary roots deserves further discussion. The former will lead to a pair of growing/decaying exponentials while the latter implies a pair of oscillatory exponentials. This is not the typical situation in boundary layer problems. Recall, for example, that in the Ekman problem [4] we have only decaying and growing exponentials. The difference in the present problem is associated with the fact that the $\tilde{\mu}\nabla^2\zeta$ term in the Euler equation represents an elastic restoring force, not a viscous damping force. Intuitively, the purely oscillatory solutions to (49) represent the elastic degree of freedom of the crust, eg. allows for the presence of the crustal shear modes in the calculation. This means that in order to properly construct the complete flow we need to keep all four solutions. Therefore we write,

$$\tilde{V}_{m+1}^0 = A_v e^{\lambda_1 \zeta} + B_v e^{-\lambda_1 \zeta} + C_v \cos(\lambda_3 \zeta) - D_v \sin(\lambda_3 \zeta) \quad (53)$$

where $\zeta = r - R_c$. Similarly,

$$\tilde{U}_m^0 = A_u e^{\lambda_1 \zeta} + B_u e^{-\lambda_1 \zeta} + C_u \cos(\lambda_3 \zeta) - D_u \sin(\lambda_3 \zeta) \quad (54)$$

As a result of eqns. (B10) and (B15), the coefficients are coupled in the following manner,

$$\tilde{\mu}\lambda_1^2(m+1)^2 \begin{Bmatrix} A_u \\ B_u \end{Bmatrix} = 4\Omega^2(m+2)Q_{m+1} \begin{Bmatrix} A_v \\ B_v \end{Bmatrix} \quad (55)$$

$$-\tilde{\mu}\lambda_3^2(m+1)^2 \begin{Bmatrix} C_u \\ D_u \end{Bmatrix} = 4\Omega^2(m+2)Q_{m+1} \begin{Bmatrix} C_v \\ D_v \end{Bmatrix} \quad (56)$$

We can now impose the boundary conditions (C1) and (C4) at $r = R_c$. These translate into

$$\lambda_1(A_v - B_v) = \lambda_3 D_v \quad (57)$$

$$\lambda_1(A_u - B_u) = \lambda_3 D_u \quad (58)$$

It is easy to see that these two relations are incompatible with (55) and (56). The only remaining option is the trivial result $D_u = D_v = 0$, which in turn means that

$$A_u = B_u, \quad \text{and} \quad A_v = B_v \quad (59)$$

Enforcing the conditions (C1) and (C4) again, this time at $r = R$, leads to

$$2\lambda_1 A_u \sinh(\lambda_1 \Delta) = \lambda_3 C_u \sin(\lambda_3 \Delta) \quad (60)$$

$$2\lambda_1 A_v \sinh(\lambda_1 \Delta) = \lambda_3 C_v \sin(\lambda_3 \Delta) \quad (61)$$

where $\Delta \equiv R - R_c$ is the crust thickness. Combining these relations with the previous ones we are led to the trivial result,

$$C_v = C_u = A_u = A_v = B_u = B_v = 0 \quad (62)$$

However, the argument that non-trivial solutions do not exist is only true provided that

$$\sin(\lambda_3 \Delta) \neq 0 \quad \Rightarrow \quad \lambda_3 \Delta \neq n\pi, \quad n \text{ integer} \quad (63)$$

This condition is obviously violated when $\Omega \rightarrow 0$. However, as we have already emphasised, we are not allowed to approach the nonrotating limit in the present framework (since for a given $\tilde{\mu}$ we always demand that $\Lambda \ll 1$). On the other hand, non-zero values of Ω that violate (63) could well be accessible. Later on in this paper we discuss the physical meaning of these particular frequencies.

We conclude that when (63) holds we must have

$$\tilde{U}_m^0 = \tilde{V}_{m+1}^0 = 0 \quad (64)$$

It also follows that $\tilde{h}_{m+1}^0 = 0$. In fact, by using eqns. (B10) and (B15) in (B20), we can prove that $\tilde{h}_{m+1}^0 = 0$ identically. Hence, somewhat unexpectedly, we conclude that at the anticipated leading order all eigenfunctions must vanish.

Before we move on, we should perhaps emphasise why we think it was worth working through the above calculation even though the end result was trivial. Basically, we wanted to highlight the exception (63), i.e., the existence of non-trivial solutions for certain parameter values. It is also worth pointing out that we would not necessarily have expected that the solution would be trivial at this level of approximation. Having said this, the result could have been inferred from the fact that the corresponding boundary conditions involve only ‘‘boundary layer’’ quantities [17].

2. First order crust flow

Having obtained a trivial result for the leading order flow, we must proceed to the next level (i.e. $\mathcal{O}(\tilde{\mu}^{1/2})$). Let us first focus on the ‘‘boundary layer’’ variables. The continuity equation (B3) gives,

$$\tilde{W}_{m+1}^1 = 0 \quad (65)$$

We can also calculate \tilde{V}_{m+1}^1 and \tilde{U}_m^1 from the radial vorticity equation (B11) and the divergence equation (B16). In view of the previous results, this last equation takes the form of eqns. (B10) and (B15) with the simple changes $\tilde{U}_m^0 \rightarrow \tilde{U}_m^1$ and $\tilde{V}_{m+1}^0 \rightarrow \tilde{V}_{m+1}^1$. The coefficients are (again) related by eqns. (55) and (56).

The relevant boundary conditions are equations (C2) and (C5) at $r = R_c$ and $r = R$. Their combination leads to,

$$A_u = -\frac{(m-1)A\lambda_3^2 R^m}{2\tilde{\mu}^{1/2} \sinh(\lambda_1 \Delta) \lambda_1 (\lambda_1^2 + \lambda_3^2)} \left[1 - \left(\frac{R_c}{R} \right)^m e^{-\lambda_1 \Delta} \right] \quad (66)$$

$$B_u = -\frac{(m-1)A\lambda_3^2 R^m}{2\tilde{\mu}^{1/2} \sinh(\lambda_1 \Delta) \lambda_1 (\lambda_1^2 + \lambda_3^2)} \left[1 - \left(\frac{R_c}{R} \right)^m e^{\lambda_1 \Delta} \right] \quad (67)$$

$$C_u = \frac{(m-1)A\lambda_1^2 R^m}{\tilde{\mu}^{1/2} \sin(\lambda_3 \Delta) \lambda_3 (\lambda_1^2 + \lambda_3^2)} \left[1 - \left(\frac{R_c}{R} \right)^m \cos(\lambda_3 \Delta) \right] \quad (68)$$

$$D_u = \frac{(m-1)A\lambda_1^2}{\tilde{\mu}^{1/2} \lambda_3 (\lambda_1^2 + \lambda_3^2)} R_c^m \quad (69)$$

Note that in the limit of a thick crust we have $e^{\lambda_1 \Delta} \gg 1$, in which case we get $A_u, A_v \rightarrow 0$ i.e. the growing exponentials are eliminated. Analogously, the two solutions that grow away from the surface will also vanish in this limit.

The remaining components V_{m+1}^1, U_m^1 and W_{m+1}^1 can be obtained from equations (B6), (B12) and (B17). Neglecting all homogeneous solutions, since we are only interested in the flow driven by the leading order r-mode, we find

$$U_m^1 = 0 \quad (70)$$

$$V_{m+1}^1 = \frac{A\sigma_1}{2\Omega\tilde{\mu}^{1/2}} (m+1) Q_{m+1} r^{m+1} \quad (71)$$

$$W_{m+1}^1 = (m+1) V_{m+1}^1 \quad (72)$$

For the pressure eigenfunctions we again find that $\tilde{h}_{m+1}^1 = 0$ identically (due to eqns. (B11), (B16) and the vanishing leading order flow). On the other hand,

$$h_{m+1}^1 = -\frac{2\Omega A Q_{m+1} \sigma_1 (2m^2 + m - 1)}{\tilde{\mu}^{1/2} (m+1)^2} r^{m+1} \quad (73)$$

The flows in the neutron star core and crust “communicate” via the interface conditions. In view of our previous results, some of these conditions reduce to trivial identities. The remaining non-trivial conditions are eqns. (C12) and (C13) which fix A and γ ,

$$A = 1, \quad \gamma = 0 \quad (74)$$

The requirement for the radial traction to vanish on the surface gives, at leading order,

$$h_{m+1}^0(R) = 0 \quad (75)$$

This familiar condition *cannot* be satisfied by our leading order solution for the simple reason that we have assumed a purely axial r-mode background flow in the core. Indeed, in order to be fully consistent, one would need to introduce $\mathcal{O}(\Omega^2)$ polar corrections, as for example in [13]. These pieces are neglected in our calculation and consequently the above surface condition should not be taken into account.

At the next order we have,

$$h_{m+1}^1 = -\frac{g_0}{R} W_{m+1}^1 \quad (76)$$

from which we obtain an expression for σ_1 ,

$$4\Omega^2 \sigma_1 (2m^2 + m - 1) = \frac{g_0}{R} \sigma_1 (m+1)^4 \quad (77)$$

The only way to satisfy this condition is by making $\sigma_1 = 0$. Hence, the leading order correction to the frequency appears at $\mathcal{O}(\tilde{\mu})$ (or higher). This result has the consequence that for the induced *core flow*,

$$V_{m+1}^1 = W_{m+1}^1 = U_m^1 = 0 \quad (78)$$

At this point we have used all available dynamical equations and boundary conditions at $\mathcal{O}(\tilde{\mu}^{1/2})$. Our results allow us to compute the crust-core slippage, a crucial quantity for the determination of the Ekman viscous dissipation rate associated with the presence of the crust [13]. Unfortunately, as we have just found, the crust-induced frequency correction is undetermined at this level. If this quantity is desired, one has to extend the calculation to the next order.

3. Second-order crust flow

We have already worked out the second order corrections to the core flow. In this section we deal with the corresponding crust corrections. To begin with, from the continuity equation (B7) we immediately obtain,

$$\tilde{W}_{m+1}^2(r) = \frac{(m+1)(m+2)}{\tilde{\mu}^{1/2}} [A_v I_1(r) + B_v I_2(r) + C_v I_3(r) - D_v I_4(r)] \quad (79)$$

where we have defined the integrals,

$$I_1(r) = \int_{R_c}^r \frac{dr'}{r'} e^{\lambda_1(r'-R_c)}, \quad I_2(r) = \int_{R_c}^r \frac{dr'}{r'} e^{-\lambda_1(r'-R_c)} \quad (80)$$

$$I_3(r) = \int_{R_c}^r \frac{dr'}{r'} \cos[\lambda_3(r'-R_c)] \quad I_4(r) = \int_{R_c}^r \frac{dr'}{r'} \sin[\lambda_3(r'-R_c)] \quad (81)$$

and we have used the continuity of the radial displacement (C9) to fix the integration constant such that $\tilde{W}_{m+1}^2(R_c) = 0$. Given this, condition (C12) requires that

$$\tilde{h}_{m+1}^2(R_c) = 0 \quad (82)$$

From eqns. (B8), (B13) and (B19) we get (again neglecting all homogeneous solutions),

$$U_m^2 = 0 \quad (83)$$

$$V_{m+1}^2 = \frac{(m+1)Q_{m+1}}{2\Omega\tilde{\mu}} \sigma_2 r^{m+1} \quad (84)$$

$$W_{m+1}^2 = (m+1)V_{m+1}^2 \quad (85)$$

Moreover, from eqns. (B23), (B24) in combination with eqns. (B18), (B7) and (B14) we obtain the pressure corrections,

$$\begin{aligned} \tilde{h}_{m+1}^2 &= -\frac{4\Omega^2 m}{(m+1)\tilde{\mu}^{1/2}} [\{Q_{m+1}A_u + A_v\}I_1(r) + \{Q_{m+1}B_u + B_v\}I_2(r) + \{Q_{m+1}C_u + C_v\}I_3(r) \\ &\quad - \{Q_{m+1}D_u + D_v\}I_4(r)] \end{aligned} \quad (86)$$

$$h_{m+1}^2 = \frac{2\Omega Q_{m+1}}{\tilde{\mu}} \frac{2-m(2m+3)}{(m+1)(m+2)} \sigma_2 r^{m+1} \quad (87)$$

The only remaining non-trivial condition (at this level of approximation) is equation (C15) which can be solved to provide the frequency correction

$$\sigma_2 = -\frac{\tilde{\mu}R^{-(m+1)}}{2\Omega Q_{m+1}} \left[\Omega_0^2 \tilde{W}_{m+1}^2(R) + \tilde{h}_{m+1}^2(R) \right] \left[\frac{2-m(2m+3)}{(m+1)(m+2)} + \frac{1}{4}(m+1)^2 \left(\frac{\Omega_0}{\Omega} \right)^2 \right]^{-1} \quad (88)$$

IV. FINAL RESULTS

After a somewhat involved calculation, we are now in a position where we can summarise the results and extract physically interesting quantities. The two most relevant quantities are i) the core-crust slippage, which enters in the estimates of the Ekman layer damping rate of core r-mode oscillations, and ii) the crust-induced frequency correction. The latter is interesting because it will unveil the presence of parameter values where our approximation scheme breaks down. As we will discuss, this happens because of the existence of distinct shear modes in the crust.

We begin by considering the extent to which the crust moves along with the core fluid. From the studies of the Ekman layer problem (see [4] for references) we know that the potential presence of a discontinuity at the core-crust interface could have significant impact on the viscous damping of a core oscillation. In principle, the role of viscosity

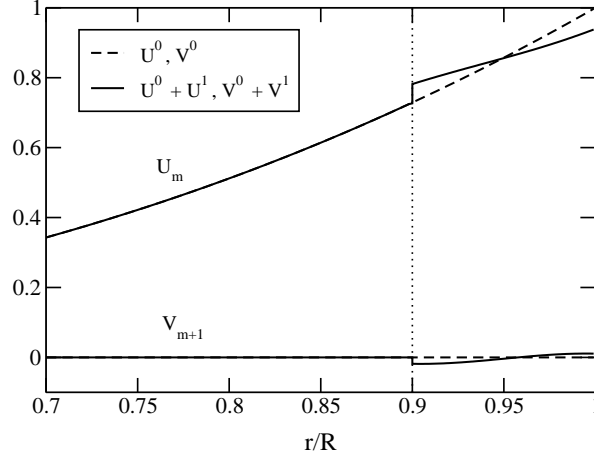


FIG. 2: Eigenfunctions U_m and V_{m+1} as functions of r/R for the $l = m = 2$ r-mode and for $\Omega = 0.3\Omega_0$, $\tilde{\mu} = 10^{-4}R^2\Omega_0^2$. Dashed and solid curves represent the background and $\mathcal{O}(\tilde{\mu}^{1/2})$ corrected eigenfunctions, respectively. The vertical dotted line represents the crust-core boundary, here taken to be at $R_c = 0.9R$.

is to smooth out any discontinuities in the inviscid solution. To date, there have been no detailed studies of the viscous problem for a star with an elastic crust. Instead the effect that the elasticity of the crust has on the Ekman damping timescale has been estimated by the core-crust “slippage” [13]. The magnitude of the relative displacement $\Delta\xi$ between the core and the crust is (obviously) given by

$$\Delta\xi = \hat{\mathbf{e}}_\theta[\xi^\theta(R_c^+) - \xi^\theta(R_c^-)] + \hat{\mathbf{e}}_\varphi[\xi^\varphi(R_c^+) - \xi^\varphi(R_c^-)] \quad (89)$$

The relative contribution of the polar and axial pieces can be seen in Fig. 2 where we show the $m = 2$ eigenfunctions for a fixed angular frequency $\Omega = 0.3\Omega_0$ (about half the Kepler break up rate) and $\tilde{\mu} = 10^{-4}R^2\Omega_0^2$. For this particular rotational frequency the axial piece is dominant, although we note that the polar piece becomes dominant once we increase the rotation rate and cross the first of the crust-core resonances discussed later. It is evident from the results shown in Fig. 2 that the corrections to the basic $l = m$ r-mode oscillation are everywhere small, thus providing credence to our approximation of truncating the multipole expansion.

The figure also clearly illustrates the discontinuity at $r = R_c$. We define the crust-core slippage \mathcal{S}_c by normalising the corresponding relative displacement with respect to the standard r-mode displacement ξ_0 . This leads to

$$\mathcal{S}_c \equiv \left| \frac{\Delta\xi}{\xi_0} \right| = \frac{1}{R_c^{m+1}} \left[|U_m(R_c^+) - U_m(R_c^-)|^2 + |V_{m+1}(R_c^+) - V_{m+1}(R_c^-)|^2 \right]^{1/2} \quad (90)$$

For a rigid crust the slippage is obviously unity, since $\Delta\xi = \xi_0$ if the fluid satisfies a no-slip condition at the base of the crust. Within the framework of the present calculation (a crust with $\Lambda \ll 1$), we can use the results for the $\mathcal{O}(\tilde{\mu}^{1/2})$ flow (Sections III E & III D) and write the leading order expression for the slippage. We have found that the corrected global r-mode eigenfunctions are,

$$U_m(r) = r^{m+1} + \Theta(\zeta) \tilde{\mu}^{1/2} [A_u e^{\lambda_1 \zeta} + B_u e^{-\lambda_1 \zeta} + C_u \cos(\lambda_3 \zeta) - D_u \sin(\lambda_3 \zeta)] \quad (91)$$

$$V_{m+1}(r) = \Theta(\zeta) \tilde{\mu}^{1/2} [A_v e^{\lambda_1 \zeta} + B_v e^{-\lambda_1 \zeta} + C_v \cos(\lambda_3 \zeta) - D_v \sin(\lambda_3 \zeta)] \quad (92)$$

$$W_{m+1}(r) = 0 + \mathcal{O}(\tilde{\mu}) \quad (93)$$

where λ_1 and λ_3 are defined by (50) and (51), and the coefficients A_u etcetera follow from (66)–(69) and (55),(56). $\Theta(\zeta)$ represents the unit step function and as before $\zeta = r - R_c$. From the above formulae we see that the discontinuity at the core-crust interface follows from

$$U_m(R_c^+) - U_m(R_c^-) = \tilde{\mu}^{1/2} \tilde{U}_m^1(R_c) = \tilde{\mu}^{1/2} (A_u + B_u + C_u) \quad (94)$$

$$V_{m+1}(R_c^+) - V_{m+1}(R_c^-) = \tilde{\mu}^{1/2} \tilde{V}_{m+1}^1(R_c) = \tilde{\mu}^{1/2} (A_v + B_v + C_v) \quad (95)$$

Then (90) becomes,

$$\mathcal{S}_c = \frac{\tilde{\mu}^{1/2}}{R_c^{m+1}} \left[|A_u + B_u + C_u|^2 + |A_v + B_v + C_v|^2 \right]^{1/2} \quad (96)$$

The way the slippage enters the r-mode problem has been discussed by LU [13] and Kinney & Mendell [18]. They find that the slippage enters quadratically in the r-mode damping formula, which leads to a revised Ekman layer timescale

$$\tau_E \rightarrow \frac{\tau_E}{\mathcal{S}_c^2} \quad (97)$$

In Fig. 3 we show the slippage as a function of Ω , for $m = 2$ and for two values of the crust thickness. The results show that a typical value is $\mathcal{S}_c \approx 0.05$. In other words, we estimate that the r-mode damping time is about a factor 400 *longer* in the case of an elastic crust that partakes in the mode oscillation than in the case of a solid crust. This estimate is in good agreement with that obtained by LU.

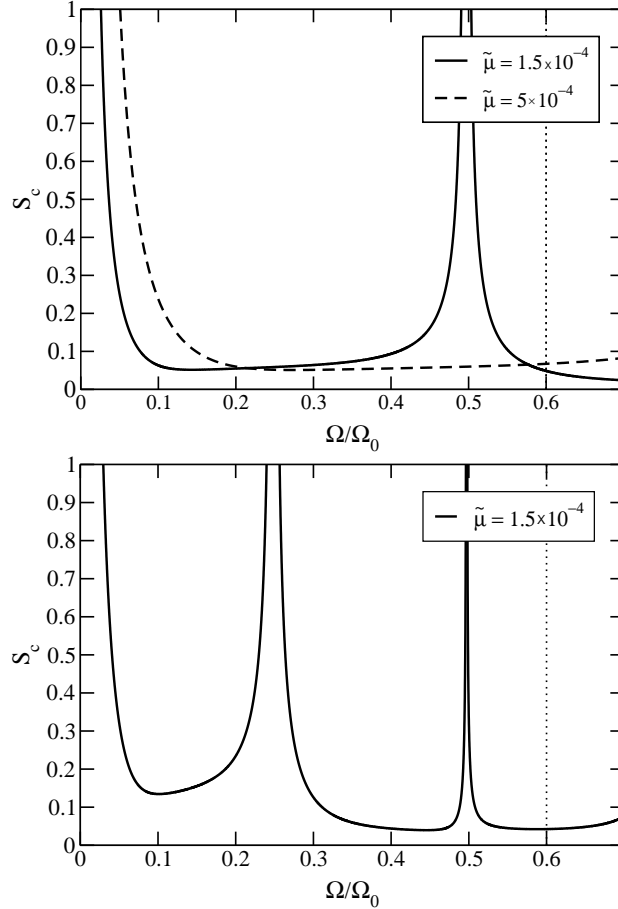


FIG. 3: The slippage \mathcal{S}_c as function of Ω/Ω_0 for $R_c = 0.9R$ (top) and $R_c = 0.8R$ (bottom). Note that the shear modulus $\tilde{\mu}$ is expressed in units of $R^2\Omega_0^2$. The vertical dotted line marks the Kepler break-up limit $\Omega_K \approx 0.6\Omega_0$. In both panels we have set $l = m = 2$ for the core r-mode oscillation.

Fig. 3 also shows the presence of resonances at certain discrete values of the angular frequency. These peaks correspond to, cf. (63),

$$\lambda_3(\Omega_n)\Delta = n\pi, \quad n \text{ integer} \quad (98)$$

Solving this condition we find the resonant frequencies,

$$\Omega_n = \tilde{\mu}^{1/2} \frac{n\pi}{2\Delta} (m+1) \sqrt{\frac{m+2}{\sqrt{\alpha}+1}} \quad (99)$$

These resonance points are apparent if we graph the frequency correction σ_2 from eqn. (88), see Fig. 4.

Clearly, the number of resonant points in the interval $\Omega \in [0, \Omega_0]$ increases with increasing crust thickness and decreasing $\tilde{\mu}$. In the vicinity of the resonances our calculation breaks down. This means that, in the vicinity of these parameter values our starting assumption that the motion is dominated by the Coriolis force and can be represented as an r-mode plus a small correction is no longer valid. One would expect this to happen when the core r-mode frequency is close to the various crust mode frequencies. In other words, the resonances in Figs. 3 and 4 indicate the occurrence of avoided crossings between core and crust modes. That this interpretation is correct is clear from the results of LU [13] and Lee & Yoshida [12]. Away from these points the mode frequency is essentially that of the core r-mode, in agreement with the numerical results of LU. Having said this, the careful reader may note that our small frequency correction differs in sign from that of LU for fast rotation. That the two results differ in this regime is not too surprising, and is likely due to LU including some higher order rotational corrections.

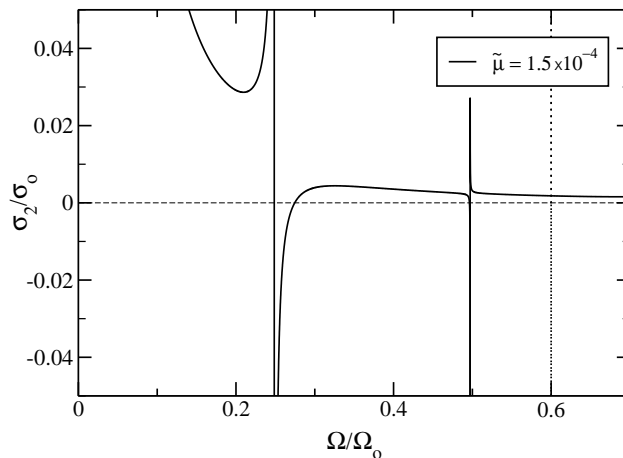


FIG. 4: Mode frequency correction σ_2 (normalised in units of the leading order frequency σ_0) as function of Ω/Ω_0 , for $l = m = 2$ and $R_c = 0.8R$. The displayed value for $\tilde{\mu}$ is in units of $R^2\Omega_0^2$ and the vertical dotted line marks the Kepler break-up limit.

V. CONCLUDING REMARKS

In this paper we have presented an analytic investigation into the interaction between an r-mode core oscillation and an idealised elastic crust for a uniform density, incompressible, rotating neutron star. The essence of our calculation is the use of boundary layer theory techniques. Our results are in agreement with previous numerical treatments of the problem [12, 13]. They also offer a more detailed description of the workings of the crust-core coupling and the emergence of resonances between the r-mode and the various crustal modes, which leads to avoided crossings in the numerical studies [12, 13]. We have provided simple analytic results for quantities like the crust-core slippage and resonant frequencies (eqns. (96) and (99)) which are of importance if one wants to estimate the viscous damping timescale for an unstable r-mode.

There are several ways that one can refine and/or expand the present analysis. Recall that we have taken the fluid to be inviscid. This assumption could be relaxed and the resulting formulation should allow a consistent computation of the viscous dissipation rate. Note that presently this dissipation has only been estimated by rescaling the Ekman damping rate with the slippage factor [13]. Other ways to improve our model would be to consider a crust with a non-uniform shear modulus (along the lines of [9]), and/or a non-spherical rotating star. Both options would make an already complicated calculation even more complicated, and one would have to approach the problem numerically.

An interesting extension would be the description of a neutron star with an elastic crust *and* a magnetic field. Based on the results from the study of the magnetic Ekman problem [18, 19] it is clear that a magnetic field may significantly change the associated r-mode damping timescale. The combination of an elastic crust and a magnetic field could well provide the most important damping mechanism for any unstable stellar modes. So far this combination has been investigated in [18], but not within a fully consistent framework. The crustal elasticity was only taken into account in the form of a slippage factor rescaling (as in (97)) the magneto-viscous dissipation rate computed for a solid boundary. Moreover, the core oscillation is assumed to be that of a normal, non-magnetic r-mode, even in the presence of strong magnetic fields which would most likely change the mode structure. There are also difficult issues of principle since the interior magnetic field structure is essentially unknown for neutron stars.

One would also have to account for the potential presence of superconducting protons in the core. A closely related problem arises from the fact that the crust is expected to be penetrated by superfluid neutrons. So far there have been no attempts to account for this feature, even though one would suspect that it could have both quantitative and qualitative impact.

From this list of outstanding problems it is clear that, after quite a lot of algebra, we have only made some small progress towards the understanding of an area where many serious challenges remain.

APPENDIX A: CORE FLOW

Using the expansion (34) in the basic equations (15), (16) and (18), when applied in the core (i.e $\mu = 0$), we obtain at first-order,

$$(m+1)\sigma_1 U_m^0 = 2\Omega Q_{m+1}[W_{m+1}^1 + (m+2)V_{m+1}^1] \quad (\text{A1})$$

$$m(m+2)Q_{m+1}[rU_m^{1'} - (m+1)U_m^1] = 2rV_{m+1}^{1'} - mrW_{m+1}^{1'} - (m+2)W_{m+1}^1 + m(m+1)(m+2)V_{m+1}^1 \quad (\text{A2})$$

$$(rW_{m+1}^1)' = (m+1)(m+2)V_{m+1}^1 \quad (\text{A3})$$

The corresponding second-order equations are,

$$(m+1)\sigma_2 U_m^0 + (m+1)\sigma_1 U_m^1 = 2\Omega Q_{m+1}[W_{m+1}^2 + (m+2)V_{m+1}^2] \quad (\text{A4})$$

$$\begin{aligned} m(m+2)Q_{m+1}[rU_m^{2'} - (m+1)U_m^2] &= \frac{\sigma_1}{2\Omega}(m+1)(m+2)[rV_{m+1}^{1'} - W_{m+1}^1] + m(m+1)(m+2)V_{m+1}^2 \\ &+ 2rV_{m+1}^{2'} - mrW_{m+1}^{2'} - (m+2)W_{m+1}^2 \end{aligned} \quad (\text{A5})$$

From eqn. (A1) we get, after using the continuity equation (18) and disregarding the homogeneous solution which becomes singular at the origin,

$$W_{m+1}^1 = \frac{\sigma_1}{2\Omega}(m+1)^2 Q_{m+1} r^{m+1} \quad (\text{A6})$$

Then eqn. (18) gives,

$$V_{m+1}^1 = \frac{\sigma_1}{2\Omega}(m+1)Q_{m+1}r^{m+1} \quad (\text{A7})$$

Solving the remaining first-order equation (A2) we get,

$$U_m^1 = \gamma r^{m+1} \quad (\text{A8})$$

where γ is a constant (since the source term in (A2) vanishes identically this is the homogeneous solution).

Similarly we find for the second-order flow,

$$W_{m+1}^2 = \frac{(m+1)^2 Q_{m+1}}{2\Omega}[\sigma_2 + \gamma\sigma_1]r^{m+1} \quad (\text{A9})$$

$$V_{m+1}^2 = \frac{(m+1)Q_{m+1}}{2\Omega}[\sigma_2 + \gamma\sigma_1]r^{m+1} \quad (\text{A10})$$

$$U_m^2 = \delta r^{m+1} \quad (\text{A11})$$

with δ another integration constant.

APPENDIX B: CRUST FLOW

In this Appendix we insert the expansion (48) in the main dynamical equations (46), (47) and (45). We group together terms of the same order in $\tilde{\mu}$ and then split those groups into ‘‘boundary layer’’ and background pieces. For

clarity, we will discuss this process in detail only for the continuity equation (which is the simplest of our equations). For the remaining dynamical equations we just list the results.

Inserting the uniform expansion in (45) we get

$$\begin{aligned} r[\tilde{W}_{m+1}^{0'} + \tilde{\mu}^a \{\tilde{W}_{m+1}^{1'} + W_{m+1}^{1'}\} + \tilde{\mu}^{2a} \{W_{m+1}^{2'} + \tilde{W}_{m+1}^{2'}\} + \tilde{\mu}^{3a} \tilde{W}_{m+1}^{3'}] &= -\tilde{W}_{m+1}^0 - \tilde{\mu}^a \{W_{m+1}^1 + \tilde{W}_{m+1}^1\} \\ -\tilde{\mu}^{2a} \{W_{m+1}^2 + \tilde{W}_{m+1}^2\} + (m+1)(m+2)[\tilde{V}_{m+1}^0 + \tilde{\mu}^a \{V_{m+1}^1 + \tilde{V}_{m+1}^1\} + \tilde{\mu}^{2a} \{V_{m+1}^2 + \tilde{V}_{m+1}^2\}] &+ \mathcal{O}(\tilde{\mu}^{3a}) \end{aligned} \quad (\text{B1})$$

Note the appearance of the seemingly “higher-order” term $\tilde{\mu}^{3a} \tilde{W}_{m+1}^{3'}$. This term is, in fact, of order $\tilde{\mu}^{2a}$ and therefore has to be included. Terms of this kind appear in other equations and the boundary conditions and one has to be aware (and cautious!) of their presence. The continuity equation splits into,

$$\tilde{W}_{m+1}^{0'} = 0, \quad \text{at } \mathcal{O}(\tilde{\mu}^{-a}) \quad (\text{B2})$$

$$r\tilde{\mu}^a \tilde{W}_{m+1}^{1'} + \tilde{W}_{m+1}^0 = (m+1)(m+2)\tilde{V}_{m+1}^0, \quad \text{at } \mathcal{O}(1) \quad (\text{B3})$$

$$rW_{m+1}^{1'} + W_{m+1}^1 + \tilde{W}_{m+1}^1 = (m+1)(m+2)(V_{m+1}^1 + \tilde{V}_{m+1}^1) - r\tilde{\mu}^a \tilde{W}_{m+1}^{2'}, \quad \text{at } \mathcal{O}(\tilde{\mu}^a) \quad (\text{B4})$$

The first of these equations immediately leads to

$$\tilde{W}_{m+1}^0 = 0 \quad (\text{B5})$$

As (B4) contains both “boundary layer” and background variables, we split it further into the two equations

$$rW_{m+1}^{1'} + W_{m+1}^1 = (m+1)(m+2)V_{m+1}^1 \quad (\text{B6})$$

$$r\tilde{\mu}^a \tilde{W}_{m+1}^{2'} = (m+1)(m+2)\tilde{V}_{m+1}^1 \quad (\text{B7})$$

The same procedure will be applied in several equations to follow. Note that it should *not* be applied in the case of boundary conditions, where one must keep “boundary layer” and core variables together. At $\mathcal{O}(\tilde{\mu}^{2a})$ the resulting background continuity equation is,

$$rW_{m+1}^{2'} + W_{m+1}^2 = (m+1)(m+2)V_{m+1}^2 \quad (\text{B8})$$

The respective “boundary layer” equation will not be needed in our calculation.

Analogously we find that the radial vorticity equation implies (28), with $\sigma \rightarrow \sigma_0$, at leading order. To derive the next order equation (which should govern the leading order flow) we need to determine the exponent a . Potential terms for this equation are,

$$\begin{aligned} \tilde{\mu}(m+1)\tilde{U}_m^{0''} + \left\{ \sigma_0\sigma_1(m+1) + \frac{1}{r^2}\tilde{\mu}m(m+1)^2 \right\} (U_m^0 + \tilde{U}_m^0) \\ - 2\sigma_0\Omega Q_{m+1}(m+2)\tilde{V}_{m+1}^0 + (m+1)\tilde{\mu}^{1+a}\tilde{U}_m^{1''} = 0 \end{aligned} \quad (\text{B9})$$

After some experimentation we find that $a = 1/2$ is the appropriate choice (other possibilities do not lead to consistent solutions). Then we get at $\mathcal{O}(1)$;

$$-\tilde{\mu}(m+1)\tilde{U}_m^{0''} + 2\Omega\sigma_0 Q_{m+1}(m+2)\tilde{V}_{m+1}^0 = 0 \quad (\text{B10})$$

while at $\mathcal{O}(\tilde{\mu}^{1/2})$ we have

$$\begin{aligned} -\tilde{\mu}(m+1)\tilde{U}_m^1 + 2\Omega\sigma_0 Q_{m+1}[(m+2)\tilde{V}_{m+1}^1 + \tilde{W}_{m+1}^1] &= (m+1)\tilde{\mu}^{-1/2}\sigma_0\sigma_1\tilde{U}_m^0 \\ &- 2\Omega\sigma_1\tilde{\mu}^{-1/2}(m+2)Q_{m+1}\tilde{V}_{m+1}^0 \end{aligned} \quad (\text{B11})$$

$$2\Omega\tilde{\mu}^{1/2}Q_{m+1}[W_{m+1}^1 + (m+2)V_{m+1}^1] = (m+1)\sigma_1 U_m^0 \quad (\text{B12})$$

One level up, at $\mathcal{O}(\tilde{\mu})$, we have

$$\begin{aligned} \tilde{\mu}^{-1/2}(m+1)(\sigma_1^2 + \sigma_0\sigma_2)U_m^0 + (m+1)\sigma_1\sigma_0U_m^1 &= -\tilde{\mu}^{1/2}(m+1)\left[U_m^{0''} - \frac{1}{r^2}m(m+1)U_m^0\right] \\ + 2\Omega\sigma_1Q_{m+1}[W_{m+1}^1 + (m+2)V_{m+1}^1] + 2\Omega\sigma_0Q_{m+1}\tilde{\mu}^{1/2}[W_{m+1}^2 + (m+2)V_{m+1}^2] \end{aligned} \quad (\text{B13})$$

and

$$\tilde{\mu}^{3/2}(m+1)\tilde{U}_m^{2''} = 2\Omega\sigma_0Q_{m+1}\tilde{\mu}^{1/2}[\tilde{W}_{m+1}^2 + (m+2)\tilde{V}_{m+1}^2] + 2\Omega\sigma_1Q_{m+1}(m+2)\tilde{V}_{m+1}^1 - (m+1)\sigma_0\sigma_1\tilde{U}_m^1 \quad (\text{B14})$$

In the case of the ‘‘divergence’’ equation the leading order background flow is governed by the standard result (29), with $U_m \rightarrow U_m^0$. The $\mathcal{O}(\tilde{\mu}^{-1/2})$, $\mathcal{O}(\tilde{\mu}^0)$ and $\mathcal{O}(\tilde{\mu}^{1/2})$ equations are,

$$(m+1)(m+2)[\tilde{\mu}\tilde{V}_{m+1}^{0'''} + \sigma_0^2\tilde{V}_{m+1}^{0'}] - 2\Omega\sigma_0m\tilde{V}_{m+1}^{0'} - 2\Omega\sigma_0m(m+2)Q_{m+1}\tilde{U}_m^{0'} = 0 \quad (\text{B15})$$

$$\begin{aligned} (m+1)(m+2)[r\tilde{\mu}^{3/2}\tilde{V}_{m+1}^{1'''} + \sigma_0^2r\tilde{\mu}^{1/2}\tilde{V}_{m+1}^{1'} + 2\sigma_0\sigma_1r\tilde{V}_{m+1}^{0'} + 2m\Omega\sigma_0\tilde{V}_{m+1}^0] - 2\Omega\sigma_0mr\tilde{\mu}^{1/2}[\tilde{V}_{m+1}^{1'} + \tilde{W}_{m+1}^{1'}] \\ - 2\Omega\sigma_1mr\tilde{V}_{m+1}^{0'} - 2\Omega\sigma_0m(m+2)Q_{m+1}[r\tilde{\mu}^{1/2}\tilde{U}_m^{1'} - (m+1)\tilde{U}_m^0] - 2\Omega\sigma_1m(m+2)Q_{m+1}r\tilde{U}_m^{0'} = 0 \end{aligned} \quad (\text{B16})$$

and

$$\begin{aligned} (m+1)(m+2)\sigma_0^2[rV_{m+1}^{1'} - W_{m+1}^1] + 2\Omega\sigma_0m(m+1)(m+2)V_{m+1}^1 = 2\Omega\sigma_0mr[V_{m+1}^{1'} + W_{m+1}^1] \\ + 2\Omega\sigma_0m(m+2)Q_{m+1}[rU_m^{1'} - (m+1)U_m^1] + 2\Omega\sigma_1\tilde{\mu}^{-1/2}m(m+2)Q_{m+1}[rU_m^{0'} - (m+1)U_m^0] \end{aligned} \quad (\text{B17})$$

$$\begin{aligned} (m+1)(m+2)r[\tilde{\mu}^{3/2}\tilde{V}_{m+1}^{2'''} + \tilde{\mu}^{1/2}\sigma_0^2\tilde{V}_{m+1}^{2'}] - 2\Omega m\sigma_0\tilde{\mu}^{1/2}r[\tilde{V}_{m+1}^{2'} + \tilde{W}_{m+1}^{2'}] = 2\Omega m(m+2)\sigma_0Q_{m+1}\tilde{\mu}^{1/2}r\tilde{U}_m^{2'} \\ + 2\Omega\sigma_1mr\tilde{V}_{m+1}^{1'} + 2\Omega m(m+2)Q_{m+1}[\sigma_1r\tilde{U}_m^{1'} - \sigma_0(m+1)\tilde{U}_m^1] - 2\Omega m(m+1)(m+2)\sigma_0\tilde{V}_{m+1}^1 \end{aligned} \quad (\text{B18})$$

respectively. Finally, the $\mathcal{O}(\tilde{\mu})$ equation is,

$$\begin{aligned} m(m+2)Q_{m+1}[rU_m^{2'} - (m+1)U_m^2] = \frac{\sigma_1}{2\Omega}(m+1)(m+2)[rV_{m+1}^{1'} - W_{m+1}^1] + 2rV_{m+1}^{2'} \\ + m(m+1)(m+2)V_{m+1}^2 - [mrW_{m+1}^{2'} + (m+2)W_{m+1}^2] \end{aligned} \quad (\text{B19})$$

To complete the required set of equations, we consider the θ -component of the Euler equation which leads to the pressure eigenfunction (42) at leading order. Meanwhile the $\mathcal{O}(\tilde{\mu}^0)$ and $\mathcal{O}(\tilde{\mu}^{1/2})$ equations give

$$\begin{aligned} \tilde{h}_{m+1}^0 &= \frac{1}{(m+2)Q_{m+1}}[-m\sigma_0\{\sigma_0 - 2\Omega Q_{m+1}^2\}\tilde{U}_m^0 - m\tilde{\mu}\tilde{U}_m^{0''} + \sigma_0Q_{m+1}\{(m+2)\sigma_0 + 2m\Omega\}\tilde{V}_{m+1}^0 \\ &+ \tilde{\mu}(m+2)Q_{m+1}\tilde{V}_{m+1}^{0''}] \end{aligned} \quad (\text{B20})$$

and

$$\begin{aligned} h_{m+1}^1 &= \frac{1}{(m+2)Q_{m+1}}[-2m\sigma_1\tilde{\mu}^{-1/2}\{\sigma_0 - \Omega Q_{m+1}^2\}U_m^0 - m\sigma_0\{\sigma_0 - 2\Omega Q_{m+1}^2\}U_m^1 \\ &+ \sigma_0Q_{m+1}\{\sigma_0(m+2) + 2m\Omega\}V_{m+1}^1] \end{aligned} \quad (\text{B21})$$

$$\begin{aligned} \tilde{h}_{m+1}^1 &= \frac{1}{(m+2)Q_{m+1}}[-m\tilde{\mu}\tilde{U}_m^{1''} + (m+2)Q_{m+1}\tilde{\mu}\tilde{V}_{m+1}^{1''} - m\sigma_0\{\sigma_0 - 2\Omega Q_{m+1}^2\}\tilde{U}_m^1 \\ &+ \sigma_0Q_{m+1}\{\sigma_0(m+2) + 2m\Omega\}\tilde{V}_{m+1}^1 - 2m\sigma_1\tilde{\mu}^{-1/2}\{\sigma_0 - \Omega Q_{m+1}^2\}\tilde{U}_m^0 \\ &+ 2\sigma_1\tilde{\mu}^{-1/2}Q_{m+1}\{(m+2)\sigma_0 + m\Omega\}\tilde{V}_{m+1}^0] \end{aligned} \quad (\text{B22})$$

The $\mathcal{O}(\tilde{\mu})$ equations are,

$$h_{m+1}^2 = \frac{1}{(m+2)Q_{m+1}} \left[-m\sigma_0\{\sigma_0 - 2\Omega Q_{m+1}^2\}U_m^2 - \frac{2m\sigma_1}{\tilde{\mu}^{1/2}}\{\sigma_0 - \Omega Q_{m+1}^2\}U_m^1 - \frac{m}{\tilde{\mu}}\{\sigma_1^2 + 2\sigma_0\sigma_2 - 2\Omega\sigma_2 Q_{m+1}^2\}U_m^0 \right. \\ \left. + \sigma_0 Q_{m+1}\{\sigma_0(m+2) + 2m\Omega\}V_{m+1}^2 + \frac{2\sigma_1}{\tilde{\mu}^{1/2}}Q_{m+1}\{\sigma_0(m+2) + 2m\Omega\}V_{m+1}^1 \right] \quad (\text{B23})$$

and

$$\tilde{h}_{m+1}^2 = \frac{1}{(m+2)Q_{m+1}} \left[-m\sigma_0\{\sigma_0 - 2\Omega Q_{m+1}^2\}\tilde{U}_m^2 - \frac{2m\sigma_1}{\tilde{\mu}^{1/2}}\{\sigma_0 - \Omega Q_{m+1}^2\}\tilde{U}_m^1 + \sigma_0 Q_{m+1}\{\sigma_0(m+2) + 2m\Omega\}\tilde{V}_{m+1}^2 \right. \\ \left. + \frac{2\sigma_1}{\tilde{\mu}^{1/2}}Q_{m+1}\{\sigma_0(m+2) + 2m\Omega\}\tilde{V}_{m+1}^1 - m\tilde{\mu}\tilde{U}_m^{2''} + \tilde{\mu}(m+2)Q_{m+1}\tilde{V}_{m+1}^{2''} \right] \quad (\text{B24})$$

APPENDIX C: BOUNDARY CONDITIONS

In this Appendix we expand the boundary conditions (22)–(26) with respect to $\tilde{\mu}$.

From the conditions pertaining to the tangential traction at both $r = R_c$ and $r = R$ we obtain,

$$\tilde{U}_m^{0'} = 0 \quad , \quad \text{at } \mathcal{O}(\tilde{\mu}^{-1/2}) \quad (\text{C1})$$

$$r[U_m^{0'} + \tilde{\mu}^{1/2}\tilde{U}_m^{1'}] = 2(U_m^0 + \tilde{U}_m^0) \quad , \quad \text{at } \mathcal{O}(\tilde{\mu}^0) \quad (\text{C2})$$

$$r[U_m^{1'} + \tilde{\mu}^{1/2}\tilde{U}_m^{2'}] = 2(U_m^1 + \tilde{U}_m^1) \quad , \quad \text{at } \mathcal{O}(\tilde{\mu}^{1/2}) \quad (\text{C3})$$

$$\tilde{V}_{m+1}^{0'} = 0 \quad , \quad \text{at } \mathcal{O}(\tilde{\mu}^{-1/2}) \quad (\text{C4})$$

$$r\tilde{\mu}^{1/2}\tilde{V}_{m+1}^{1'} = 2\tilde{V}_{m+1}^0 \quad , \quad \text{at } \mathcal{O}(\tilde{\mu}^0) \quad (\text{C5})$$

$$r[V_{m+1}^{1'} + \tilde{\mu}^{1/2}\tilde{V}_{m+1}^{2'}] = 2(V_{m+1}^1 + \tilde{V}_{m+1}^1) - (W_{m+1}^1 + \tilde{W}_{m+1}^1) \quad , \quad \text{at } \mathcal{O}(\tilde{\mu}^{1/2}) \quad (\text{C6})$$

Continuity of the radial displacement at $r = R_c$ demands,

$$W_{m+1}^0(R_c^-) = W_{m+1}^0(R_c^+) + \tilde{W}_{m+1}^0(R_c^+) \quad (\text{C7})$$

$$W_{m+1}^1(R_c^-) = \tilde{\mu}^{1/2}[W_{m+1}^1(R_c^+) + \tilde{W}_{m+1}^1(R_c^+)] \quad (\text{C8})$$

$$W_{m+1}^2(R_c^-) = \tilde{\mu}[W_{m+1}^2(R_c^+) + \tilde{W}_{m+1}^2(R_c^+)] \quad (\text{C9})$$

Note that the first of these conditions is trivially satisfied since we are assuming that the leading order flow is purely axial.

Finally, from the radial traction conditions at the crust-core interface and the surface we get,

$$h_{m+1}^0(R_c^-) = h_{m+1}^0(R_c^+) + \tilde{h}_{m+1}^0(R_c^+) \quad (\text{C10})$$

$$h_{m+1}^1(R_c^-) = \tilde{\mu}^{1/2}[h_{m+1}^1(R_c^+) + \tilde{h}_{m+1}^1(R_c^+)] \quad (\text{C11})$$

$$h_{m+1}^2(R_c^-) = \tilde{\mu}[h_{m+1}^2(R_c^+) + \tilde{h}_{m+1}^2(R_c^+)] - 2\tilde{\mu}^{3/2}\frac{\tilde{W}_{m+1}^{1'}(R_c^+)}{R_c^+} \quad (\text{C12})$$

,and

$$h_{m+1}^0 + \tilde{h}_{m+1}^0 = 0 \quad (\text{C13})$$

$$h_{m+1}^1 + \tilde{h}_{m+1}^1 = -\frac{g_0}{R}[W_{m+1}^1 + \tilde{W}_{m+1}^1] \quad (\text{C14})$$

$$h_{m+1}^2 + \tilde{h}_{m+1}^2 = -\frac{g_0}{R}[W_{m+1}^2 + \tilde{W}_{m+1}^2] + \frac{2\tilde{\mu}^{1/2}}{R}\tilde{W}_{m+1}^{1'} \quad (\text{C15})$$

respectively.

ACKNOWLEDGMENTS

This work was supported by PPARC through grant number PPA/G/S/2002/00038. NA also acknowledges support from PPARC via Senior Research Fellowship no PP/C505791/1.

- [1] N. Andersson, ApJ **502**, 708 (1998)
- [2] J.L. Friedman and S.M. Morsink, ApJ **502**, 714 (1998)
- [3] N. Andersson and K.D. Kokkotas, Int. J. Mod. Phys. **D10**, 381 (2001)
- [4] K. Glampedakis and N. Andersson, MNRAS **371**, 1311 (2006)
- [5] P. Haensel, K.P. Levenfish and D.G. Yakovlev, Astron. Astrophys. **381**, 1080 (2002)
- [6] A. Reisenegger and A. Bonacic, Phys. Rev. Lett **91**, 201103 (2003)
- [7] M. Nayyar and B.J. Owen, Phys. Rev. D **73**, 084001 (2006)
- [8] N. Andersson, G.L. Comer and K. Glampedakis, Nucl. Phys. A **763**, 212 (2005)
- [9] U. Lee and T.E. Strohmayer, Astron. Astrophys. **311**, 155 (1996)
- [10] P.N. McDermott, H.M. Van Horn and C.J. Hansen, ApJ **325**, 725 (1988)
- [11] T.E. Strohmayer, ApJ, **372**, 573 (1991)
- [12] S. Yoshida and U. Lee, ApJ **546**, 1121 (2001)
- [13] Y. Levin and G. Ushomirsky, MNRAS, **324**, 917 (2001)
- [14] F. Douchin and P. Haensel, Astron. Astrophys. **380**, 151 (2001)
- [15] K.H. Lockitch and J.L. Friedman, ApJ **521**, 764 (1999)
- [16] L.D. Landau and E.M. Lifshitz, *Theory of Elasticity*, Course of Theoretical Physics Vol. 7, 3rd edition (Butterworth, Heinemann, Oxford 1999).
- [17] C.M. Bender and S.A. Orszag, *Advanced Mathematical Methods for Scientists and Engineers* (McGraw-Hill International Editions, 1978)
- [18] J. Kinney and G. Mendell, Phys. Rev. D **67** 024032 (2003)
- [19] G. Mendell, Phys. Rev. D **64**, 044009 (2001)